ChemComm

COMMUNICATION

View Article Online
View Journal

Reactivity of a Ru(III)–hydroxo complex in substrate oxidation in water†

Cite this: DOI: 10.1039/c4cc07488b

Shingo Ohzu, Tomoya Ishizuka, Hiroaki Kotani and Takahiko Kojima*

Received 22nd September 2014,
Accepted 13th October 2014

DOI: 10.1039/c4cc07488b

www.rsc.org/chemcomm

A mononuclear Ru^{III}–OH complex oxidizes substrates such as hydroquinones in water through a pre-equilibrium process based on adduct formation by hydrogen bonding between the Ru^{III}–OH complex and the substrates. The reaction mechanism switches from hydrogen atom transfer to electron transfer depending on the oxidation potential of substrates.

Substrate oxidation reactions of organic substrates with iron(III)- or other trivalent metal–hydroxo complexes have been intensively investigated due to not only the relevance of the active species in biological oxidation catalysed by lipoxygenases[1] but also the interest in high reactivity despite the relatively low oxidation state of the metal centres.[2] The oxidation reactions with synthetic metal(III)–hydroxo complexes as oxidants have been mainly performed in organic solvents.[2–4] In contrast, the reactivity of trivalent metal–hydroxo complexes for substrate oxidation in water has yet to be clarified. Additionally, it has not been well elucidated so far how the reorganization energy (λ) of electron transfer (ET) for a metal complex affects the reactivity in substrate oxidation performed by the metal complex.[5]

High-valent ruthenium complexes have also been intensively investigated as active species of substrate oxidation reactions both in organic solvents[6] and water.[7] Ruthenium complexes exhibit highly reversible redox behaviours to exhibit high catalytic turnover numbers. The valences of the ruthenium centres of the oxidants employed so far are +IV[8] for most cases, +V[9] or +VI[10] for several cases, whereas there are few reports on a Ru^{III}–hydroxo complex as an active species for substrate oxidation in water. Herein, we report detailed kinetic studies on substrate oxidation reactions with a Ru^{III}–hydroxo complex in water (Fig. 1).

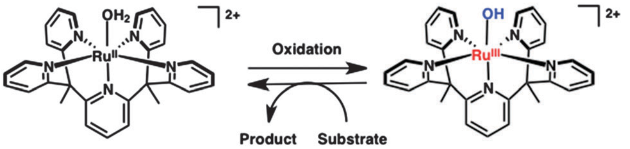

1 2

Fig. 1 Generation of $[Ru^{III}(OH)(PY5Me_2)]^{2+}$ (**2**) from $[Ru^{II}(PY5Me_2)(H_2O)]^{2+}$ (**1**) and oxidation of substrates with **2**.

A Ru^{II}–aqua complex with a pentadentate poly-pyridyl ligand, 2,6-bis{1,1-bis(2-pyridyl)ethyl}pyridine ($PY5Me_2$),[11] $[Ru^{II}(PY5Me_2)(OH_2)]^{2+}$ (**1**), was synthesized by treatment of $[Ru^{II}Cl(PY5Me_2)]^{+}$ (see Fig. S1 and S2 in ESI†) with $AgPF_6$ in water. Characterization of **1** was made by using ^1H NMR spectroscopy, ESI-TOF-MS spectrometry and elemental analysis.[12] The pK_a values of **1** were determined in Britton–Robinson (B–R) buffer,[13] based on the UV-Vis spectral change (Fig. S3 in the ESI†), to be pK_{a1} = 11.0. Cyclic and differential-pulse voltammograms (CV and DPV) of **1** were measured in B–R buffer at various pH values and the Pourbaix diagram was drawn based on the results of the electrochemical measurements and the pK_a values determined (Fig. 2). In the pH range and within the potential window measured, no wave due to a Ru^{III}/Ru^{IV} redox couple was observed (Fig. S4 in the ESI†). In the Pourbaix diagram, the potential of the oxidation step decreases as the solution pH increases with an inclination of −52 mV per pH in the pH range of 1.8–11.0. The result indicates that the $1e^-$ and $1H^+$ processes of the Ru^{II}–OH_2 give complex **2** in the pH range. The BDE value of **1** was estimated to be 77 kcal mol^{-1}, on the basis of the redox potential and the pK_a value.[12]

Electrochemical oxidation of **1** (0.5 mM) at +1.3 V *vs.* SCE in B–R buffer (pH 1.8) clearly exhibited the one-step spectral change due to generation of **2** (Fig. S5 in the ESI†). The UV-Vis spectral change in the course of the electrochemical oxidation of **1** ended at the elementary electric charge of 0.097 C, which matched the theoretical value for the one-electron oxidation of the Ru^{II} species to form the corresponding Ru^{III} complex (0.093 C). The ESI-MS spectrum was measured for the aqueous solution of **2** generated

---

Department of Chemistry, Faculty of Pure and Applied Sciences, University of Tsukuba, 1-1-1 Tennoudai, Tsukuba, Ibaraki 305-8571, Japan. E-mail: kojima@chem.tsukuba.ac.jp

† Electronic supplementary information (ESI) available: Experimental details of syntheses and characterization of compounds, summary of optical absorption and redox potential, and cyclic and differential-pulse voltammograms. CCDC 1022568. For ESI and crystallographic data in CIF or other electronic format see DOI: 10.1039/c4cc07488b

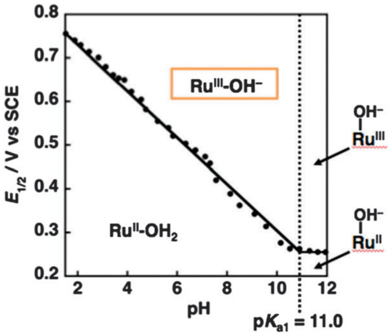

Fig. 2 A plot of redox potential against solution pH (Pourbaix diagram) for **1** in B–R buffer. Potential values were determined relative to SCE (as 0 V) at room temperature.

by the electrochemical oxidation of **1** and a peak cluster was observed at m/z = 281.17 with the feature of a divalent cation, which was ascribed to the signal of $[\mathbf{2}\text{–}2PF_6]^{2+}$ (Fig. S6 in the ESI†).

To elucidate the reactivity of **2** in the oxidation of organic substrates, we performed kinetic analyses of the quantitative oxidation of 2,5-dichlorohydroquinone (H_2QCl_2) with electrochemically generated **2**.[14] The reactions were performed in the presence of an excess amount of H_2QCl_2 (25–150 mM) relative to 2 (0.5 mM) in B–R buffer (pH 1.8) and the rate constants were determined by UV/Vis spectroscopy to trace the increase of absorption due to the Ru^{II} species at 380 nm at various temperatures (Fig. 3a). All the time courses of the absorbance changes obeyed the first-order kinetics and the pseudo-first-order rate constants (k_{obs}) were determined at various concentrations of H_2QCl_2. In the oxidation of H_2QCl_2 with 2, the pseudo-first-order rate constants were saturated against the concentration of H_2QCl_2 at all the temperatures examined (Fig. 3b and Fig. S8 in the ESI†), indicating the existence of pre-equilibrium processes prior to the oxidation.[7]

We also conducted kinetic analyses for oxidation of two more substrates, 2,3,5,6-tetrafluoro-hydroquinone (H_2QF_4) and ascorbic acid (AS). The kinetic analyses for oxidation of the three substrates allowed us to determine the equilibrium constants (K) for the pre-equilibrium processes and the first-order rate constants (k) at various temperatures (Fig. S8 in the ESI†). Based on the plots of the equilibrium constants and the rate constants relative to the inverse of the reaction temperatures (T^{-1}) (van't Hoff plots and Eyring plots, respectively), the thermodynamic parameters for the pre-equilibrium processes and the activation parameters for the oxidation reactions were determined respectively (Table 1 and Fig. S9 and S10 in the ESI†). The enthalpy changes (ΔH°) of the pre-equilibrium process show a tendency to become more negative upon increasing the acidity of the hydroxy groups of substrates,[15,16] indicating hydrogen bonding between the oxygen of **1** and the hydroxy group of a substrate as the driving force of the adduct formation. In addition, the relatively small activation parameters suggest that the pre-equilibrium process between **2** and the substrate afforded an appropriate arrangement for hydrogen-atom transfer (HAT) (Fig. 4).

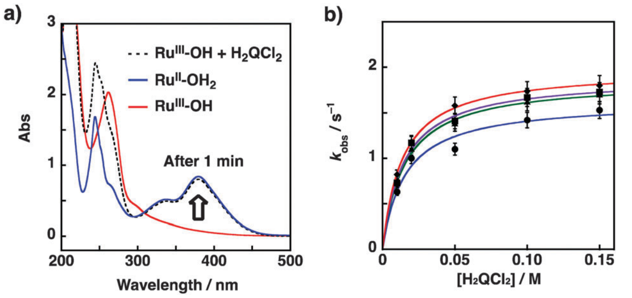

Fig. 3 (a) Spectral changes during the oxidation of H_2QCl_2 with 2 (0.5 mM) in B–R buffer (pH 1.8) at 297 K. The initial spectrum of **2** before adding the substrate (red) and the final spectrum after the oxidation reaction (black dotted line) and the spectrum of **1** (blue) are shown. (b) Pseudo-first-order kinetic analysis for the oxidation of H_2QCl_2 with **2** as the oxidant (0.5 mM) in B–R buffer (pH 1.8) at 305 (red), 297 (purple), 289 (green), and 281 K (blue).

Table 1 Oxidation potential and thermodynamic parameters for the pre-equilibrium processes and activation parameters for the oxidation reactions of substrates with **2**

Substrate	E_{ox} [a]	pK_{a1}	$\Delta H^{\ddagger}$ [b]	$\Delta S^{\ddagger}$ [c]	ΔH° [b]	ΔS° [c]
H_2QF_4	+0.61	3.90[d]	8.0	−18	−7.6	10
H_2QCl_2	+0.51	4.96[d]	4.0	−28	−4.2	20
AS	+0.37	5.17[e]	12	1.4	−1.4	22
H_2QCl	+0.06	9.21[d]	6.6	−3.4	1.3	27
H_2QF	+0.13	9.42[d]	6.1	−7.3	1.7	27
H_2Q	−0.05	9.95[d]	7.4	10.5	1.4	26

[a] V *vs.* SCE. [b] kJ mol^{-1}. [c] J mol^{-1} K^{-1}. [d] Ref. 15. [e] Ref. 16.

To obtain further information on the oxidation process, studies of the kinetic isotope effects (KIE) for oxidation reactions of substrates with **2** were conducted at 297 K. The KIE values were determined to be the ratio of the rate constants (k_H/k_D) for the oxidation reactions of substrates using H_2O (k_H) and D_2O (k_D) as solvents (Fig. S11 in the ESI†). The reactions were monitored by UV-Vis spectroscopy to track the increase of the absorbance due to the Ru^{II} species formed. The oxidation of substrates showed KIE values for the hydroxy group to be 1.7 for H_2QCl_2 and H_2QF_4, and 1.2 for AS (Table 2).[17] The KIE values for oxidation with the three substrates indicate that the hydrogen atom abstraction from the hydroxy group is involved in the rate-determining step.

Four more substrates, hydroquinone (H_2Q), 2-chloro-hydroquinone (H_2QCl), 2-fluoro-hydroquinone (H_2QF), and 2-methoxy-hydroquinone ($H_2Q(OMe)$), having lower redox potentials (−0.05 V *vs.* SCE for H_2Q, +0.06 V for H_2QCl, +0.13 V for H_2QF, and −0.18 V for $H_2Q(OMe)$) than those of the other three substrates (+0.51 V for H_2QCl_2 and +0.61 V for H_2QF_4 and +0.37 V for AS *vs.* SCE),

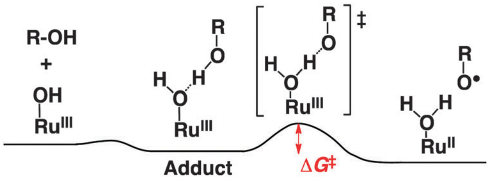

Fig. 4 Schematic energy diagram of the intermediates for the substrate oxidation with **2** in water. R represents aryl or alkyl groups of the substrates.

Table 2 Kinetic data for oxidation reactions with **2** in B–R buffer at 297 K

Substrate	k_H (s^{-1})	k_D (s^{-1})	k_H/k_D
$H_2Q(OMe)$	56	52	1.1
H_2Q	53	48	1.1
H_2QCl	13	13	1.0
H_2QF	10	8.8	1.1
H_2QCl_2	1.9	1.1	1.7
H_2QF_4	1.7	1.0	1.7
AS	2.1	1.7	1.2

were utilized as substrates for the oxidation reactions with **2** (Fig. S12 in the ESI†).[14] The three substrates also exhibited the pre-equilibrated adduct formation (Fig. S8 in the ESI†) and the ΔH° values also showed a similar dependence on the pK_{a1} values of the substrates (Table 1). The larger rate constants for the oxidation of H_2Q, H_2QF and H_2QCl compared to those for the oxidation of the other three substrates probably derive from the lower redox potential of substrates (Table 1 and Fig. S8 in the ESI†). In addition, the oxidation reactions of H_2Q, H_2QF, H_2QCl and $H_2Q(OMe)$ exhibited no KIE (1.1 for H_2Q, 1.0 for H_2QCl, 1.1 for H_2QF, and 1.1 for $H_2Q(OMe)$, and see Fig. S11 in the ESI†), indicating that the oxidation reactions of the four substrates proceed through electron transfer (ET) from substrates to **2**.[5]

A plot of the logarithm of the rate constants at 297 K relative to the driving force of ET ($-\Delta G_{ET}$) was made to shed light on the change of the reaction mechanism from HAT to ET in the substrate oxidation reactions by **2** (Table S1 in the ESI†). As shown in Fig. 5, substrates having smaller $-\Delta G_{ET}$ (<0.5 eV) are oxidized by the HAT mechanism with small driving-force dependence. In stark contrast, those having larger $-\Delta G_{ET}$ (>0.5 eV) are oxidized by the ET mechanism and the rate constants fit a Marcus plot[18] for intramolecular non-adiabatic ET with λ of 1.31 eV and the electronic coupling matrix element (V) of 0.0011 cm^{-1}.[12] The switching point of the reaction mechanisms is estimated to be located at $-\Delta G_{ET}$ = 0.51 eV. The λ value and the $-\Delta G_{ET}$ of the switching point for the reaction mechanisms of substrate oxidation with **2** are larger than those of other high-valent metal complexes that are proposed to oxidize substrates through ET.[5] These results indicate that the λ value becomes larger and ET from substrates to an oxidant becomes more difficult in a polar solvent like water.[19]

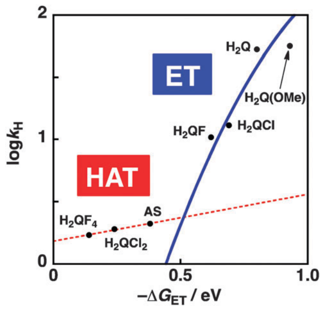

Fig. 5 A plot of the logarithm of rate constants relative to the driving forces of ET ($-\Delta G_{ET}$). All the data were determined at 297 K in B–R buffer (pH 1.8). The blue line is drawn by using eqn (3) in the ESI† with λ = 1.31 eV and the red dashed line indicates a linear dependence of log k_H on $-\Delta G_{ET}$ for HAT reactions.

In conclusion, we have synthesized a novel Ru^{III}–OH complex, **2**, with $PY5Me_2$ as a pentadentate polypyridyl ligand by electrochemical oxidation of the corresponding Ru^{II}–aqua complex in B–R buffer. We have experimentally elucidated the reactivity of a Ru^{III}–OH complex in substrate oxidation in water on the basis of kinetic analysis. The oxidation reactions of substrates by **2** in water involve a pre-equilibrium process based on adduct formation by hydrogen bonding between the Ru^{III}–OH complex and the substrates.[20] The oxidation reaction mechanism with **2** in water switches from HAT to ET, depending on the oxidation potential of substrates employed. The switching of the reaction mechanisms for substrate oxidation reactions has never been observed without assistance by Lewis-acidic metal ions to control the reduction potential of the oxidant.[5] Here, mechanistic switching resulting from the remarkable increase of the λ value of ET in water is observed, which enables the slow ET from substrates showing positive $-\Delta G_{ET}$. This work may provide a valuable basis to elucidate the reactivity of a trivalent metal–hydroxo complex in oxidation reactions of organic substrates in water in relevance to those catalysed by lipoxygenases.

Notes and references

1 (*a*) T. M. Jonsson, H. Glickman, S. J. Sun and J. P. Klinman, *J. Am. Chem. Soc.*, 1996, **118**, 10319; (*b*) C.-C. Hwang and C. B. Grissom, *J. Am. Chem. Soc.*, 1994, **116**, 795; (*c*) E. R. Lewis, E. Johansen and T. R. Holman, *J. Am. Chem. Soc.*, 1999, **121**, 1395.
2 (*a*) C. R. Goldsmith and T. D. P. Stack, *Inorg. Chem.*, 2006, **45**, 6048; (*b*) C. R. Goldsmith, A. P. Cole and T. D. P. Stack, *J. Am. Chem. Soc.*, 2005, **127**, 9904.
3 P. J. Donoghue, J. Tehranchi, C. J. Cramer, R. Sarangi, E. I. Solomon and W. B. Tolman, *J. Am. Chem. Soc.*, 2011, **133**, 17602.
4 (*a*) C. R. Goldsmith and T. D. P. Stack, *Inorg. Chem.*, 2006, **45**, 6048; (*b*) C. R. Goldsmith, A. P. Cole and T. D. P. Stack, *J. Am. Chem. Soc.*, 2005, **127**, 9904.
5 (*a*) Y. Morimoto, J. Park, T. Suenobu, Y.-M. Lee, W. Nam and S. Fukuzumi, *Inorg. Chem.*, 2012, **51**, 10025; (*b*) J. Park, Y. Morimoto, Y.-M. Lee, W. Nam and S. Fukuzumi, *J. Am. Chem. Soc.*, 2011, **133**, 5236; (*c*) J. Park, Y. Morimoto, Y.-M. Lee, W. Nam and S. Fukuzumi, *Inorg. Chem.*, 2014, **53**, 3618.
6 (*a*) T. J. Meyer, *Acc. Chem. Res.*, 1989, **22**, 163; (*b*) S. L.-F. Chan, Y.-H. Kan, K.-L. Yip, J.-S. Huang and C.-M. Che, *Coord. Chem. Rev.*, 2011, **255**, 899; (*c*) M. Zhou and R. H. Crabtree, *Chem. Soc. Rev.*, 2011, **40**, 1875.
7 (*a*) T. Ishizuka, S. Ohzu and T. Kojima, *Synlett*, 2014, 1667; (*b*) Y. Hirai, T. Kojima, Y. Mizutani, Y. Shiota, K. Yoshizawa and S. Fukuzumi, *Angew. Chem., Int. Ed.*, 2008, **47**, 5772; (*c*) T. Kojima, Y. Hirai, T. Ishizuka, Y. Shiota, K. Yoshizawa, K. Ikemura, T. Ogura and S. Fukuzumi, *Angew. Chem., Int. Ed.*, 2010, **49**, 8449; (*d*) S. Ohzu, T. Ishizuka, Y. Hirai, H. Jiang, M. Sakaguchi, T. Ogura, S. Fukuzumi and T. Kojima, *Chem. Sci.*, 2012, **3**, 3421.
8 (*a*) W. K. Seok and T. J. Meyer, *J. Am. Chem. Soc.*, 1988, **110**, 7358; (*b*) P. Neubold, K. Wieghardt, B. Nuber and J. Weiss, *Angew. Chem., Int. Ed. Engl.*, 1988, **27**, 933.
9 (*a*) M. M. T. Khan, D. Chatterjee, R. R. Merchant, P. Paul, S. H. R. Abdi, D. Srinivas, M. R. H. Siddiqui, M. A. Moiz, M. M. Bhadbhade and K. Venkatasubramanian, *Inorg. Chem.*, 1992, **31**, 2711; (*b*) X. Guan, S. L.-F. Chan and C.-M. Che, *Chem. – Asian J.*, 2013, **8**, 2046.
10 S. Perrier, T. C. Lau and J. K. Kochi, *Inorg. Chem.*, 1990, **29**, 4190.
11 E. A. Ünal, D. Wiedemann, J. Seiffert, J. P. Boyd and A. Grohmann, *Tetrahedron Lett.*, 2012, **53**, 54.
12 See the ESI†.
13 R. Wang, J. G. Vos, R. H. Scmehl and R. Hage, *J. Am. Chem. Soc.*, 1992, **114**, 1964.

14 The products of oxidation reactions of hydroquinones were confirmed to be the corresponding quinones by ^{1}H NMR spectroscopy. See Fig. S7 in the ESI†.

15 X.-Q. Zhu, C.-H. Wang and H. Liang, *J. Org. Chem.*, 2010, **75**, 7240.

16 Y.-N. Wang, K.-C. Lau, W. W. Y. Lam, W.-L. Man, C.-F. Leung and T.-C. Lau, *Inorg. Chem.*, 2009, **48**, 400.

17 Small KIE values in HAT reactions have been reported: (*a*) T. Osako, K. Ohkubo, M. Taki, Y. Tachi, S. Fukuzumi and S. Itoh, *J. Am. Chem. Soc.*, 2003, **125**, 11027; (*b*) S. C. Weatherly, I. V. Yang and H. H. Thorp, *J. Am. Chem. Soc.*, 2001, **123**, 1236.

18 (*a*) R. A. Marcus and N. Sutin, *Biochim. Biophys. Acta*, 1985, **811**, 265; (*b*) R. A. Marcus, *Angew. Chem., Int. Ed. Engl.*, 1993, **32**, 1111.

19 S. Fukuzumi, K. Ohkubo, T. Suenobu, K. Kato, M. Fujitsuka and O. Ito, *J. Am. Chem. Soc.*, 2001, **123**, 8459.

20 T. Ishizuka, S. Ohzu, H. Kotani, Y. Shiota, K. Yoshizawa and T. Kojima, *Chem. Sci.*, 2014, **5**, 1429.